

THE PALAEOLITHIC SITE SIMA DE LAS PALOMAS DE TEBA, SOUTHERN SPAIN – SITE FORMATION PROCESSES AND CHRONOSTRATIGRAPHY

M. Kehl (1), C. Burow(1), P. Cantalejo(2), S. Domínguez-Bella(3), J.J. Durán(4), F. Henselowsky(1), N. Klasen(1), F.J. Medianero(2), J. Ramos(5), K. Reicherter(6), C. Schmidt(7), G.-C. Weniger(8)

- (1) Institute of Geography, University of Cologne, Albertus Magnus Platz, 50923 Köln, Germany; kehlm@uni-koeln.de
- (2) Escuela Taller Parque Guadalteba y Red Patrimonio Guadalteba, Área de Arqueología, Consorcio Guadalteba, Ctra. Campillos-Málaga, km 11, Campillos, 29320 Málaga, Spain
- (3) Área de Cristalografía y Mineralogía, Facultad de Ciencias, Universidad de Cádiz, Campus Río San Pedro, Puerto Real, 11003 Cádiz, Spain
- (4) Instituto Geológico y Minero de España (IGME), C/ Ríos Rosas, 23, 28003 Madrid, Spain
- (5) Área de Prehistoria, Departamento de Historia, Geografía y Filosofía, Facultad de Filosofía y Letras, Universidad de Cádiz, Avda Gómez Ulla, s/n, 11003 Cádiz, Spain
- (6) Neotectonics and Natural Hazards, RWTH Aachen University, Lochnerstrasse 4-20, 52056 Aachen, Germany
- (7) Chair of Geomorphology, Department of Geography, University of Bayreuth, 95440 Bayreuth, Germany
- (8) Stiftung Neanderthal Museum, Talstrasse 300, 40822 Mettmann, Germany

Abstract (The Palaeolithic site Sima de las Palomas de Teba, Southern Spain –Site formation processes and chronostratigraphy): The rockshelter sequence consists of 6 m thick stone-rich silty clay loam including several archaeological levels with artefacts of Mousterian affinity, bone and charcoal. Stratigraphy and site formation processes were characterised by sedimentological, geochemical and micromorphological investigations. Sediments were dated using IRSL and OSL and the time of the last heating of burnt silex using TL. At the base of the sequence, sediment units 10 and 9 are in-situ deposits recording intensive occupation. Luminescence dating places these layers either before 33 ka (IRSL, OSL) or before 43 ka (TL). The occupation ends with a rockfall (unit 8), followed by archaeologically sterile sediments (unit 7). Mousterian occupation is again documented in scattered artefacts of units 6 to 4 which might be affected by reworking. IRSL age estimates indicated sediment deposition before 15 ka. The sequence ends with a dung rich Holocene layer including a fragment of a human mandible dated to 4032 ± 39 BP. Overall, the sequence represents an important new site for studying the presence of Neanderthals in Southern Spain.

Key words: Neanderthal occupation, site formation processes, micromorphology, luminescence dating

INTRODUCTION

The Sima de las Palomas de Teba is a vertical limestone chasm, at least 9 m deep and located about 100 m below the crest of a south facing slope within Cretaceous limestone of the Sierra de Teba-Peñarrubia in the Province of Málaga. The Sima belongs to the uppermost part of a doline forming a nexus to the karst complex of the Cueva de Las Palomas which extends downslope towards the gorge of Tajo del Molino (Medianero et al., 2011).

The south wall of the Sima consists of about 6 m thick silty clay loam with varying admixtures of rocks and boulders as well as artefacts of Mousterian affinity, bones, charcoal and molluscs. In former times, the chasm was probably completely filled with sediments before unknown excavators dug out the artefact rich material and heaped it on the land surface of the doline. The sediment profile exposed has not been investigated in detail before, but offers the perspective to study Mousterian occupation in the Guadalteba district.

Information recovered from profile analysis so far indicate a series of Middle Palaeolithic occupations that appear to be interrupted by at least one occupation hiatus. Human presence at the site is fading out in the upper part of the sequence. Reoccupation after the Middle Palaeolithic does not start before the Holocene.

Modern climate of the area is semiarid Mediterranean (Csa acc. to KOEPPEN). Mean annual air temperature

range from 15 to 17.5 °C and mean annual precipitation is between 400 and 700 mm (Atlas Climático Ibérico, sine ano). Limited data is available on the climate conditions during the past, but marine cores from the Alboran Sea and terrestrial archives in Southern Spain clearly reflect changes between dry and cool, and moist and humid conditions during the time of Middle Palaeolithic occupation. For example, pollen spectra from the Middle Palaeolithic layers 19 to 14 at Bajondillo document changes between steppic and forested landscapes (López-Sáez et al., 2007). Lithological, palynological and geochemical records of the Fuentillejo Maar (Vegas et al., 2010, Ortiz et al., 2013) also suggest major climate driven changes in the lake catchment during the Last Glacial involving pulses of dry and cold climatic conditions.

Our objectives were to define stratigraphic units and shed light on site formation processes in the rockshelter. In addition, we aimed at providing a chronological framework for sediment accumulation and occupation of the rockshelter.

METHODS

The central part of the exposure was cleaned and sketched. The locations of silex, bone, charcoal and mollusk shells were recorded for the entire width of the exposure (Figure 1). The sequence was described in the field and samples were extracted along a sediment column (sedimentology, geochemistry) and from selected sediment units

(luminescence dating, micromorphology). Laboratory investigations included determination of the granulometric composition of the siliceous fine fraction (< 2mm in diameter, destruction of carbonate with HCl) using a laser diffractometer (Beckman laser Coulter LS13320) after dispersion with 0.01 M $\text{Na}_4\text{P}_2\text{O}_7 \cdot 10\text{H}_2\text{O}$. Major and trace element composition of press pills prepared using the silt and clay fraction (< 63 μm) were measured with a Spectro Xepos HE x-ray fluorescence (XRF) spectrometer. Volumetric magnetic susceptibility was determined on sieved air-dried samples using a Bartington field spectrometer equipped with the MS2F sensor. Soil colour was measured for homogenised soil samples in triplicates with a spectrophotometer (Konica Minolta CM-5) by detecting the diffused reflected visible light in the 360 to 740 nm range under standardised observation conditions (2° Standard Observer, Illuminant C). The spectral information was converted into Munsell values and into the CIELAB Colour Space system (CIE 1976) using the Software SpectraMagic NX (Konica Minolta).

A series of 15 thin sections, (60 mm x 80 mm in length, ~30 μm thick) were prepared from 11 sediment monoliths extracted from different units (Figure 1) and wrapped in plaster bandages. Thin section preparation was carried out by Th. Beckmann, Schwülper-Lagesbüttel, Germany. Descriptions of thin sections followed Stoops (2003).

For estimating the time of sedimentation with luminescence dating techniques five sediment samples were extracted using opaque metal tubes. Infrared stimulated luminescence (IRSL) and elevated temperature post-IR IRSL (pIR-IRSL; Buylaert et al. 2009, Thiel et al. 2011) on coarse-grained feldspar and polymineralic fine grains and optically stimulated luminescence (OSL) on coarse- and fine-grained quartz were conducted on three samples, while additional dating is in progress. All measurements followed the standard single-aliquot regenerative-dose (SAR) procedure after Murray and Wintle (2003). Dating the time of last heating of burnt silex was carried out on five samples, which were found to be suitable for thermoluminescence (TL) dating. As the surrounding sediment could not be sampled for determination of external dose rates, it was assumed that the dose rates measured for the IRSL/OSL samples CP 1 and CP 2 are representative for sediments of unit 9 and 10. Further details on analytical TL procedures are given in Schmidt (2013).

RESULTS

At the base of the sequence, sediment **units 10 and 9** contained abundant Mousterian artefacts of mode III-type, as well as bone and charcoal fragments. These units were characterised by low sediment brightness (L^* -values), high magnetic susceptibility (MS) and comparatively high P contents (Fig. 2). Thin sections showed horizontal orientation of elongated bone and limestone fragments (Fig. 3A) and a high degree of compaction. The sediment was particularly rich in well preserved angular bone fragments and moderately rounded bone sand (Fig. 3B). Fragments of surface seals (Fig. 3C, Pagliai and Stoops, 2010) indicated that the sediment gradually accumulated

during occupation of the site. TL ages of the burnt artefacts were between 43 and 96 ka, if 1 sigma error ranges are taken into account (Fig. 1). IRSL and OSL dating resulted in ages between 33 and 56 ka (Tab. 1).

Large blocks within **unit 8** derived from partial roof collapse. The fine material in between the blocks and overlying **unit 7** had higher L^* values, lower MS and finer grain size distribution than the sediment of unit 9. At the interface of unit 7 with overlying unit 6, the K/Rb ratio significantly increased suggesting an increase in weathering intensity in unit 6. Units 8 and 7 appeared to contain no artefacts (Fig. 1), but very few pieces of silex, bone and charcoal were found under the microscope within thin section CP M6. Micromorphology also revealed a lower degree of structure development and a lighter colour of the groundmass in comparison to unit 9, the latter probably being related to lower contents of organic matter.

Units 6 to 4 were moderately rich in artefacts of Mousterian affinity and documented a considerably lower occupation density than units 10 and 9. In the field, no distinct boundaries between these units were detected, but laboratory results showed differences between the layers. For example, unit 6 had comparatively coarse median grain sizes, elevated P contents and low L^* values (Fig. 2). Unit 5 represents a transitional layer towards unit 4, the uppermost Pleistocene deposit. All thin sections from these units were characterised by loosely packed silty to clayey groundmass with abundant limestone fragments (Fig. 3B) but few bone, silex or charcoal. Although micromorphological features do not suggest major differences, thin section CP M10 from the top of unit 4 showed a more clearly developed subangular blocky structure and darker groundmass. Features characteristic for units 9 and 10, including a high degree of compaction, horizontal clast alignment or surface seals were not found. According to IRSL/OSL age estimates, units 5 and 4 accumulated between about 31 and 15 ka (including 1 sigma error ranges).

Sediment **unit 3** had a sharp lower boundary towards unit 4, was more silty and had highest L^* values. Lithic artefacts were not recovered but the unit contained a fragment of a human mandible, which yielded a radiocarbon age of 4032 \pm 39 BP (COL 2013, on tooth). The thin section from this layer (Fig. 3C) showed characteristic calcite spherulites in the groundmass and abundant calcite grains of medium silt size (~10-20 μm in diameter) as well as remnants of herbivore coprolites (Fig. 3F).

Sediment **units 2 and 1** consisted of large boulders with interspersed grey silty matrix, comparatively rich in modern roots.

DISCUSSION

As based on micromorphological evidence reworking of sediments of units 10 and 9 appears highly unlikely. These units therefore represent in-situ archaeological levels containing Mousterian artefacts of mode III-type, which are well represented in this region of Southern Spain (Vallespi, 1986; Barroso

and De Lumley, 2006; Cortés, 2011; Ramos, 2013). The intensity of occupation apparently decreased with time, since the abundance of artefacts, bone fragments and charcoal is considerably lower in unit 9 than in unit 10. Significant redistribution of carbonates, good preservation of bone and geochemical ratios suggest weak to moderate intensity of weathering, which also holds for most other parts of the sequence. The time of occupation during accumulation of units 10 and 9 requires further investigations. The discrepancy between IRSL/OSL and TL dates is partly caused by inappropriateness of environmental dose rate determination for the silex samples. Theoretically, the time of heating silex does not need to correspond to final burial within the sediment because heated silex artefacts may have been reused.

Occupation stopped after partial roof collapse (unit 8). The few and small knapped artefacts, charcoal and bone detected under the microscope within unit 7 may have invaded the sediment by bioturbation. A clearly developed archaeological layer resembling the ones in unit 9 and 10 is not evident, and so, it appears likely, that accumulation of unit 7 took place while the cave was not occupied.

Site formation processes of the upper Mousterian levels (units 6 to 4) are of particular interest for investigating Neanderthal presence. The scattered distribution of artefacts, the general lack of depositional features such as horizontal alignment of elongated clasts or surface seals and the low degree of compaction suggest that well preserved archaeological layers are lacking. Effects of bioturbation and reworking of artefacts over a short distance by mass movement, such as slide or creep must be considered instead. This is corroborated by IRSL/OSL age estimates that are too young to correlate with Middle Palaeolithic artefacts. Independent age control by radiocarbon-dating is under way to further shed light on the chronological problem. However, significant reduction of occupation density and inconsistent dating of late Neanderthal occupations is a well known phenomenon in Southern Iberia (Schmidt et al., 2012; Wood et al., 2013). The subdivision in sediment units, as proposed here, also requires further investigation.

The Holocene deposits of unit 3 unconformably rest on the Pleistocene sequence. Variation in sedimentological parameters within this unit indicates a further subdivision, which may be unravelled during excavation. The radiocarbon date of the human mandible suggests a long depositional hiatus after accumulation of the uppermost layer of unit 4, yielding age estimates older than 15 ka (IRSL). Calcite spherulites and abundant phytoliths probably derived from dung of ovicaprines (sheep and goat), which were kept in the shelter. The large amount of microsparitic calcite crystals possibly represent degraded spherulites.

Finally, sediment **unit 2** accumulated by roof collapse and **unit 1** represents artificial deposits related to the construction of the scaffolding.

CONCLUSIONS

Overall, the sequence records various occupation events and represents an important new site for studying the presence of Neanderthals in Southern Spain. Inconsistencies in the chronological framework require further studies. The question whether units 4 to 6 containing scattered Mousterian artefacts are affected by bioturbation or by reworking of sediments, must be scrutinized during excavation of the sequence. The uppermost unit 3 may provide an interesting insight in Bronze age occupation of Guadalteba district.

Acknowledgements: We are grateful to the Consejería de Cultura de la Junta de Andalucía for authorizing our work in the framework of the project "Actividad Arqueológica Puntual en el Complejo Kárstico de Las Palomas de Teba (Málaga)". Thanks also to the institutions involved, especially, Consorcio Guadalteba, Grupo de Acción Local Guadalteba, Ayuntamiento de Ardales and Ayuntamiento de Teba.

We gratefully acknowledge XRF analyses by Jens Protze and Marianne Dohms (Division of Physical Geography of RWTH Aachen University). Dr. Eileen Eckmeier, formerly at INRES-Soil Science of Bonn University, assisted in the determination and interpretation of colour values. We thank the German Research Foundation for financial support for project C1 of the CRC806 "Our Way to Europe".

We thank students from the Escuela Taller for preparation of the profile and all fellow researchers involved in the project. Special thanks go to Eduardo Vijande, Juan Jesus Cantillo, Antonio Barrena, Antonio Cabral, Maria del Mar Espejo, Serafin Becerra and Lidia Cabello for studies of lithic products.

References

- Atlas Climático Ibérico, sine ano. Temperatura del aire y precipitación (1971-2000). Agencia Estatal de Meteorología de España and Departamento de Meteorología e Clima, Instituto de Meteorología de Portugal. 79 p.
- Barroso, C., De Lumley, H., 2006. La Grotte du Boquete de Zafarraya. Málaga, Consejería de Cultura, Junta de Andalucía, Sevilla.
- Buylaert, J.P., Murray, A.S., Thomsen, K.J., Jain, M. 2009. Testing the potential of an elevated temperature IRSL signal from K-feldspar. *Radiation Measurements* 44, 560-565.
- Cortés, M., 2011. Territorio y espacio. Paleolítico Medio y Superior en Andalucía. Un estado de la cuestión. In: Memorial Luis Siret. I Congreso de Prehistoria de Andalucía. Junta de Andalucía, Sevilla, 163-172.
- Galbraith, R.F., Roberts, R.G., Laslett, G.M., Yoshida, H., Olley, J.M. 1999. Optical dating of single and multi-grains of Quartz from Jinmium rock shelter, northern Australia: Part I, experimental design and statistical models. *Archaeometry* 41, 339-364.
- López-Sáez, J.A., López-García, P., Cortés Sánchez, M. 2007. Paleovegetación del Cuaternario reciente: Estudio arqueopalínológico. In: Cortés Sánchez, M. (Ed.), Cueva Bajondillo (Torremolinos). Secuencia cronocultural y paleoambiental del Cuaternario reciente en la Bahía de Málaga. Centro de Ediciones de la Diputación de Málaga, Junta de Andalucía, Universidad de Málaga, Fundación Cueva de Nerja y Fundación Obra Social de Unicaja, Málaga, pp 139-156.
- Medianero, F.J., Ramos, J., Palmqvist, P., Weniger, G., Riquelme, J.A., Espejo, M., Cantalejo, P., Aranda, A., Pérez-Claros, J.A., Figueirido, B., Espigares, P., Ros-Montoya, S., Torregrosa, V., Linstädter, J., Cabello, L., Becerra, S., Ledesma, P., Mevdev, I., Castro, A., Romero, M., Martínez-Navarro, B., 2011. The karst site of Las Palomas (Guadalteba County, Málaga, Spain): A preliminary study of its Middle-Late Pleistocene

archaeopaleontological record. *Quaternary International* 243, 127–136.

Murray, A.S., Wintle, A.G. 2003. The single aliquot regenerative-dose protocol: potential for improvements in reliability. *Radiation Measurements* 37, 377-381.

Ortiz, J.E., Moreno, L., Torres, T., Vegas, J., Ruiz-Zapata, B., García-Cortés, Á., Galán, L., Pérez-González, A., 2013. A 220 ka palaeoenvironmental reconstruction of the Fuentillejo maar lake record (Central Spain) using biomarker analysis. *Organic Geochemistry* 55, 85–97.

Pagliai, M., Stoops, G. 2010. Physical and Biological Surface Crusts and Seals. In: Stoops, G., Marcelino, V., Mess, F., eds: *Interpretation of Micromorphological Features of Soils and Regoliths*, Elsevier, Amsterdam, 419-440.

Ramos, J., 2013. Relationship and contacts of the Pleistocene hunter-gatherer societies with Mode III Technology between Northern Africa and the south Iberian Peninsula. In A. Pastoors, B. Auffermann (eds.): *Pleistocene foragers on the Iberian Peninsula: Their culture and environment*. *Wissenschaftliche Schriften des Neanderthal Museums* 7, Mettmann, 35-53.

Stoops, G. 2003. Guidelines for the analysis and description of soil and regolith thin sections. *Soil Science Society of America*, Madison, WI.

Schmidt, I., Bradtmöller, M., Kehl, M., Pastoors, A., Tafelmaier, Y., Weninger, B., Weninger, G.-C., 2012. Rapid climate change and variability of settlement

patterns in Iberia during the Late Pleistocene: Temporal and spatial corridors of *Homo sapiens sapiens* population dynamics during the Late Pleistocene and Early Holocene. *Quaternary International* 274, 179–204.

Schmidt, C., 2013. Luminescence dating of heated silex - Potential to improve accuracy and precision and application to Paleolithic sites. PhD thesis, University of Cologne, 300pp.

Thiel, C., Buylaert, J.-P., Murray, A., Terhorst, B., Hofer, I., Tsukamoto, S., Frechen, M. 2011. Luminescence dating of the Stratzing loess profile (Austria) – Testing the potential of an elevated temperature post-IR IRSL protocol. *Quaternary International* 234, 23-31.

Vallespi, E. (1986): *El Paleolítico inferior y medio en Andalucía*. Homenaje a Luis Siret (1934-1984). Junta de Andalucía, Sevilla, 59-66.

Vegas, J., Ruiz-Zapata, B., Ortiz, J.E., Galán, L., Torres, T., García-Cortés, Á., Gil-García, M.J., Pérez-González, A., Gallardo-Millán, J.L., 2010. Identification of arid phases during the last 50 cal. ka BP from the Fuentillejo maar-lacustrine record (Campo de Calatrava Volcanic Field, Spain). *Journal of Quaternary Science* 25, 1051–1062.

Wood, R.E., Barroso, C., Caparros, M., Jorda, J.F., Galvan Santos, B., Higham, T.F.G., 2013. Radiocarbon dating casts doubt on the late chronology of the Middle to Upper Palaeolithic transition in southern Iberia. *Proceedings of the National Academy of Sciences* 110, 2781-2786.

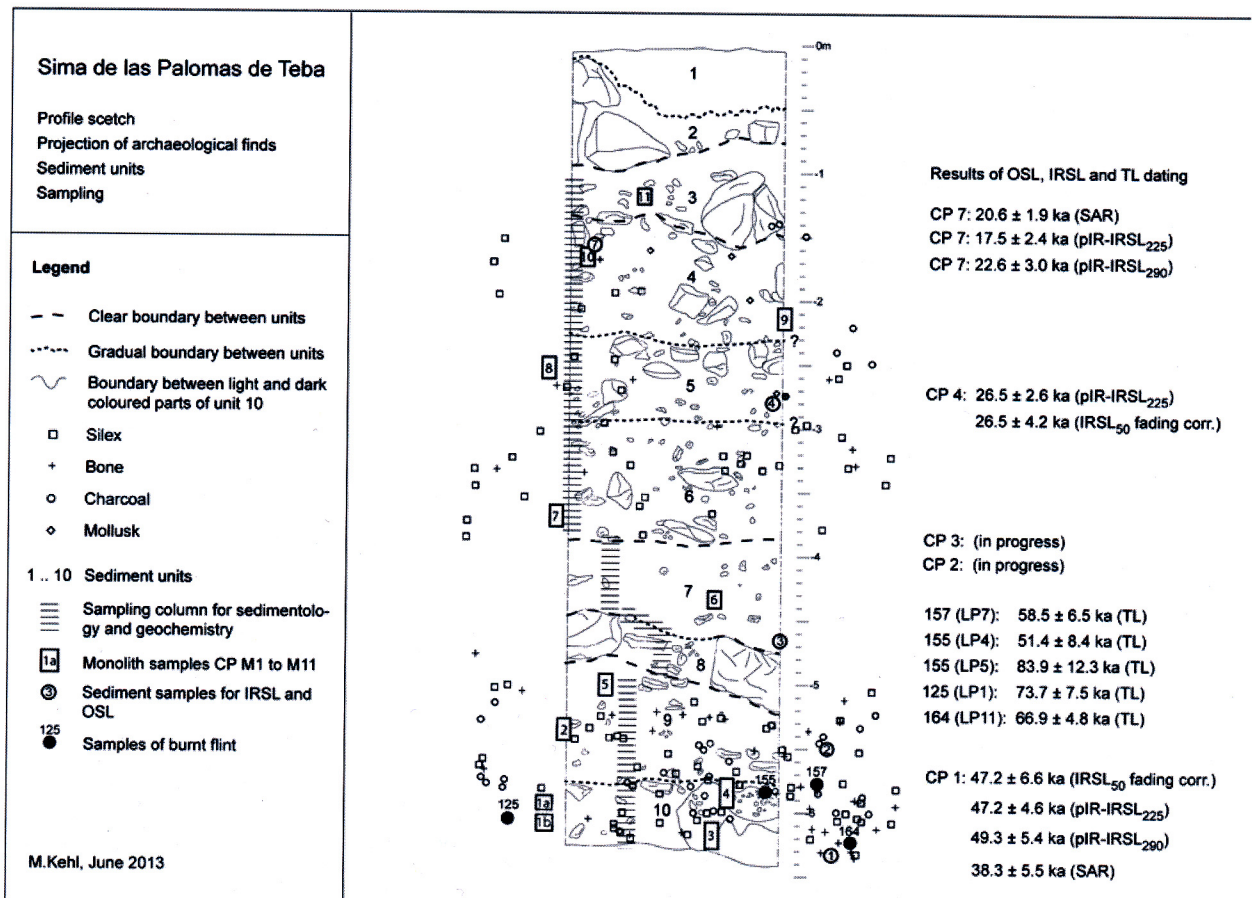


Fig. 1: The profile at Sima de las Palomas de Teba showing sediment units, distribution of archaeological finds, sampling locations and results of luminescence age estimates.

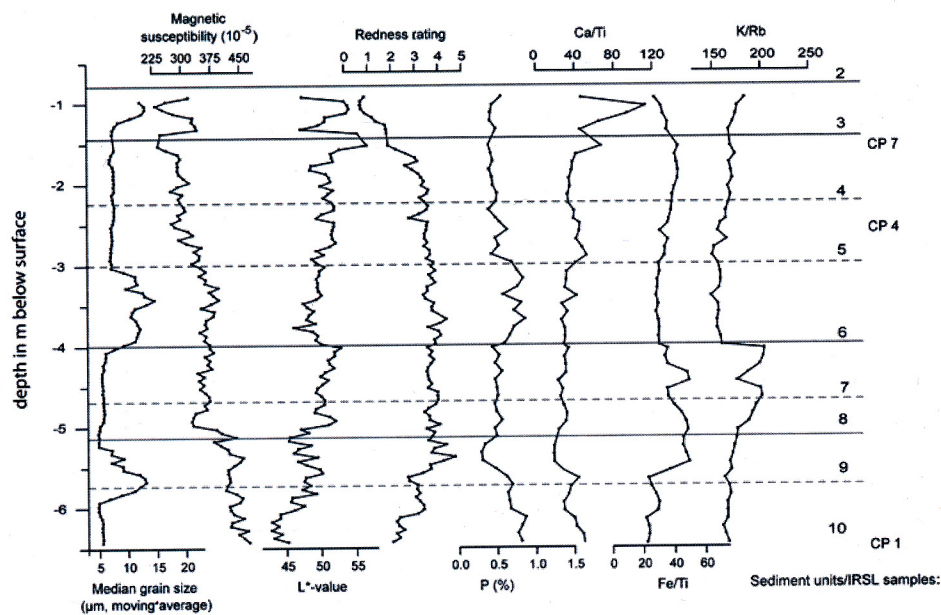


Fig. 2: Selected results of sedimentological and geochemical measurements of the samples taken from the sediment column shown in Fig. 1.

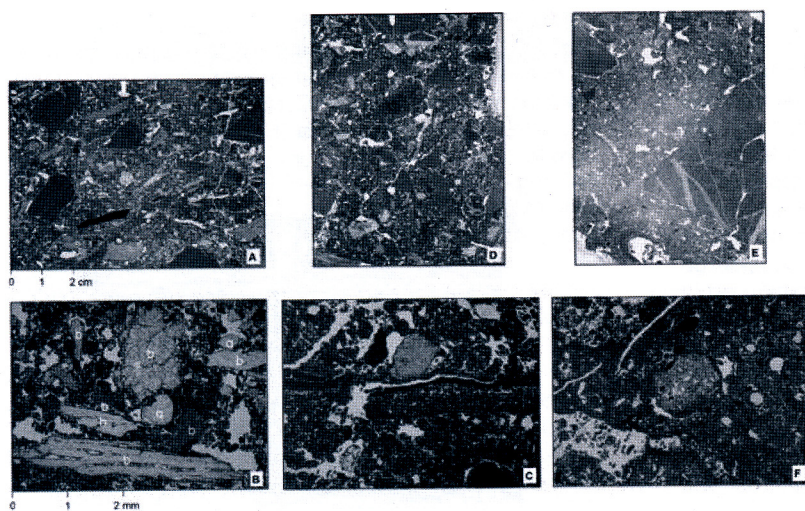


Fig. 3: Micromorphological features of selected thin sections. A: Thin section CP M3.1 from unit 10 with high amounts of bone fragments, silex and charcoal. Note horizontal alignment of elongated fragments, the comparatively high packing density and granular microstructure. B: Micrograph of CP M3.1 showing the large number of bone (b) fragments in the groundmass (plain polarized light, PPL). Note sand grains of quartz (q). C: Fragment of surface seal in CP M3.1 (PPL). D: Thin section CP M8 from unit 5. The limestone fragments appear to float in the matrix. E: Thin section CP M11 from unit 3. Few charcoal and small bones fragments, light brown micromass, very loose packing due to strong bioturbation. F: Micrograph from CP M11 with herbivore coprolite in the center. Frequent passage features and high porosity reflect bioturbation.

Table 1: Results of gamma spectrometry, dose rate calculation, equivalent dose (D_e) measurements and age estimation (based on water content of 10 ± 5 % for samples CP 1 and 6 ± 3 % for samples CP 4, CP 7). All values are shown with their 1 sigma error. IRSL₅₀ age estimates are corrected for anomalous fading. CAM = Central Age Model, COM = Common Age Model (Galbraith et al., 1999); OD = overdispersion.

Lab. Code	Sample ID	Grain size (µm)	Protocol	Water content measured (%)	Depth (m below surface)	No. of sub-samples accepted/measured	OD (%)	Dose rate (Gy/ka)	Age model	D_e (Gy)	Age (ka)
C-L3142	CP 1	100-200	IRSL ₅₀	15	6.25	13/20	20	2.67 ± 0.30	CAM	91.9 ± 6.8	47.2 ± 6.6
C-L3142	CP 1	100-200	pIR-IRSL ₂₂₅	15	6.25	14/23	6	2.67 ± 0.26	CAM	125.9 ± 6.7	47.2 ± 4.6
C-L3142	CP 1	100-200	pIR-IRSL ₂₉₀	15	6.25	13/19	19	2.67 ± 0.29	CAM	131.6 ± 9.6	49.3 ± 5.3
C-L3142	CP 1	4-11	SAR	15	6.25	10/10	0	2.40 ± 0.34	COM	92.0 ± 4.8	38.3 ± 3.9
C-L3143	CP 4	100-200	IRSL ₅₀	7	2.70	11/19	25	2.81 ± 0.33	CAM	57.8 ± 5.3	26.5 ± 4.2
C-L3143	CP 4	100-200	pIR-IRSL ₂₂₅	7	2.70	17/28	18	2.82 ± 0.28	CAM	74.6 ± 5.0	26.5 ± 2.6
C-L3368	CP 7	4-11	pIR-IRSL ₂₂₅	8	1.55	10/10	2.7	2.27 ± 0.30	CAM	39.8 ± 2.0	17.5 ± 2.3
C-L3368	CP 7	4-11	pIR-IRSL ₂₉₀	8	1.55	9/9	0	2.28 ± 0.30	COM	51.6 ± 2.6	22.6 ± 3.0
C-L3368	CP 7	4-11	SAR	8	1.55	22/22	0	1.96 ± 0.18	COM	40.6 ± 2.1	20.6 ± 1.9